

# Synthesis and Characterization of Hydroxyapatite Using Precursor Extracted from Seashell Waste

Posharani Saravanan, Sharrmitah Saravanakumar, Rozainita Rosley\*

*Department of Science and Mathematics, Centre for Diploma Studies,  
Universiti Tun Hussein Onn Malaysia, Pagoh Higher Education Hub, 84600 Pagoh, Johor, MALAYSIA*

\*Corresponding Author: [rozainita@uthm.edu.my](mailto:rozainita@uthm.edu.my)

DOI: <https://doi.org/10.30880/mari.2024.05.01.008>

## Article Info

Received: 01 September 2023

Accepted: 10 December 2023

Available online: 31 January 2024

## Keywords

Seashell Waste, Hydroxyapatite,  
Calcination, Biomaterial

## Abstract

Shells can cause environmental problems due to microbial and bacterial activity in the shells. However, this waste contains  $\text{CaCO}_3$  which can be converted into hydroxyapatite (HAp). HAp is bioactive and biocompatible and has been used for several biomedical applications. Synthesizing HAp from natural sources can contribute significantly towards natural resource management, health care and waste utilization amongst others. The focus of research is to make the whole process eco-friendly, economical and minimal waste generating. The synthesis of HAp was carried out through a calcination method with different weights of seashell powder where the precursor material was reacted with a calcium and phosphate-containing solution under controlled conditions. The synthesized hydroxyapatite samples were characterized using various analytical techniques. X-ray diffraction (XRD) analysis was performed to determine the phase purity and crystal structure of the synthesized hydroxyapatite. Scanning electron microscopy (SEM) was employed to study the morphology and particle size of the HAp crystals. Additionally, Fourier-transform infrared spectroscopy (FTIR) was used to identify the functional group present in the HAp structure. From the various analytical techniques, 30 g of seashell powder showed the highest peak in XRD analysis and FTIR analysis displayed the broad and strong absorption of HAp. The HAp derived from seashell waste was synthesized and validated from the results. The synthesized HAp possesses desirable characteristics for biomedical applications, making it a promising material for future research and development in the field of regenerative medicine and biomaterials.

## 1. Introduction

One of the most adaptable types of biomaterials now accessible is hydroxyapatite (HAp), which has the chemical formula  $\text{Ca}_{10}(\text{PO}_4)_6(\text{OH})_2$ . Its chemical makeup is extremely similar to that of human bone in terms of the calcium-phosphate (Ca/P) ratio and other organic substances. Distinctive features of any material to be considered a biomaterial include bioactive, non-seiditious, biocompatible, osteoconductive, harmless and non-immunogenic [1].

Human bone, enamel, and dentine are mostly composed of this calcium phosphate salt. HAp is calcium phosphate, or CaP, which is the name for a group of minerals that include calcium cations ( $\text{Ca}^{2+}$ ), orthophosphate, metaphosphate, or pyrophosphate anions as hydrogen and hydroxide ions on occasion [2]. Luckily all these

© 2024 UTHM Publisher. All rights reserved.

This is an open access article under the CC BY-NC-SA 4.0 license.



features are present in HAp since it resembles with calcium phosphates components of human bone and has proven biocompatibility with these tissues, so it is extensively utilized for biomedical applications such as the renovation of skull faults, repair of massive bone imperfection, bone tissue engineering, elimination of heavy metals and more importantly in drugs delivery [3].

The objectives of this research are to synthesize HAp via chemical precipitation by calcination method. The second, is to characterize synthesized HAp using Energy Dispersive Spectroscopy (EDX), X-ray Diffraction (XRD), Fourier Transform Infrared (FTIR), and Scanning Electron Microscope (SEM).

## 2. Materials and Methods

### 2.1 Materials

Seashells were purchased from an online Shoppe platform. Potassium Dihydrogen Phosphate ( $\text{KH}_2\text{PO}_4$ ) was obtained from the UTHM Laboratory. Distilled water in this experiment was obtained directly from the laboratory.

### 2.2 Synthesis of HAp Powder

The seashells were cleaned and boiled to remove organic material and impurities that were attached to it. The seashells were soaked in water for several days in a large pot with water at room temperature in prior for boiling. The water was brought to a rolling boil for approximately ten minutes to avoid damaging the seashells. Then, the seashells were removed carefully and let them cool down on a towel.

The cleaned seashells were dried in the oven for 1 hour at  $110\text{ }^\circ\text{C}$  to isolate any contaminants. The cleaned seashells were crushed using the ball mill into small particle sizes and grinning into fine powder particles. Then, it was sieved using a sieve shaker to get a powder size ranging between  $71$  to  $125\text{ }\mu\text{m}$ .

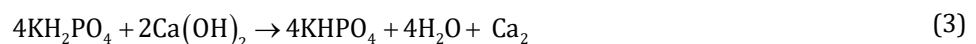
The seashell powder was calcinated at  $800\text{ }^\circ\text{C}$  for 3 hours to extract CaO. The calcination process converts the calcium carbonate ( $\text{CaCO}_3$ ) from seashell to calcium oxide (CaO) by releasing carbon dioxide ( $\text{CO}_2$ ) as shown in (1).



HAp powders were synthesized by precipitation with calcium hydroxide ( $\text{Ca}(\text{OH})_2$ ) and  $\text{H}_3\text{PO}_4$ . The  $\text{Ca}(\text{OH})_2$  was created from the combination of CaO and water ( $\text{H}_2\text{O}$ ) as shown in (2).



Next, the wet slurry precipitation technique was used to produce HAp. The CaO was dissolved in water to obtain  $\text{Ca}(\text{OH})_2$ . The amount of powder used will be different to test which is the suitable weight of  $\text{Ca}(\text{OH})_2$  to produce Hydroxyapatite. Afterwards, 5 drops of  $\text{KH}_2\text{PO}_4$  (Potassium dihydrogen phosphate) solution was dropped into  $\text{Ca}(\text{OH})_2$  solutions to form Hydroxyapatite [4] as shown in (3).



The reaction time was fixed to 4 hours to get the best solution. The mixture was then centrifuged at 3000 rpm for 10 minutes to get the milky white precipitate referred to as hydroxyapatite. The solution was filtered with filter paper. The methods to produce HAp powder are shown in Fig. 1.

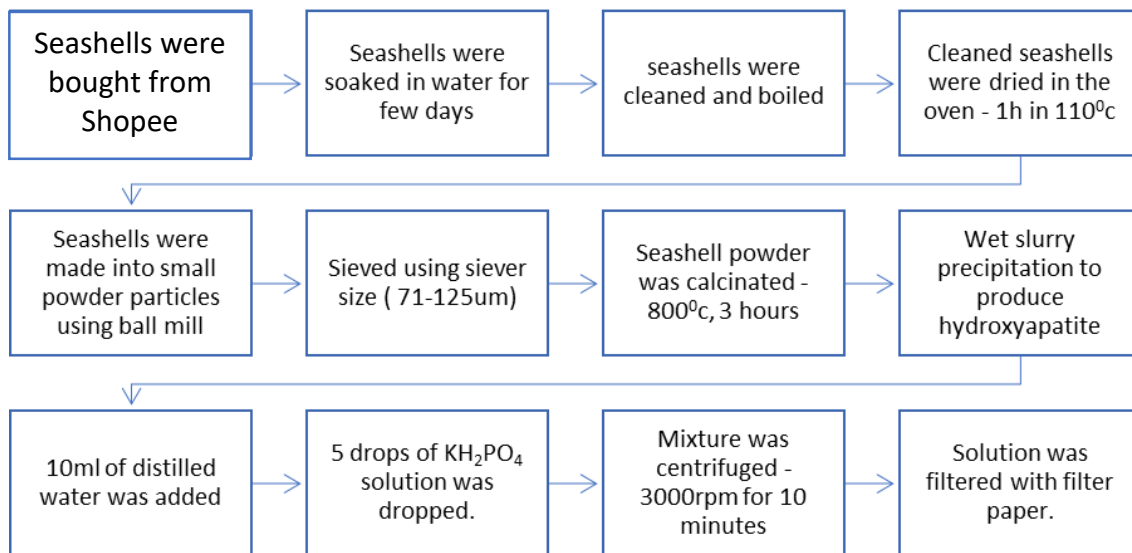


**Fig.1** Methods to produce HAp powder

### 3. Results and Discussion

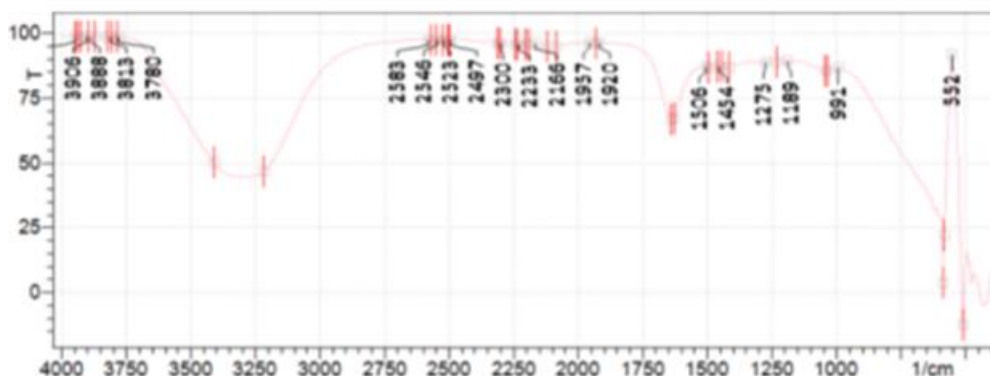
#### 3.1 Fourier-Transform Infrared Absorbance Spectra (FTIR) Analysis

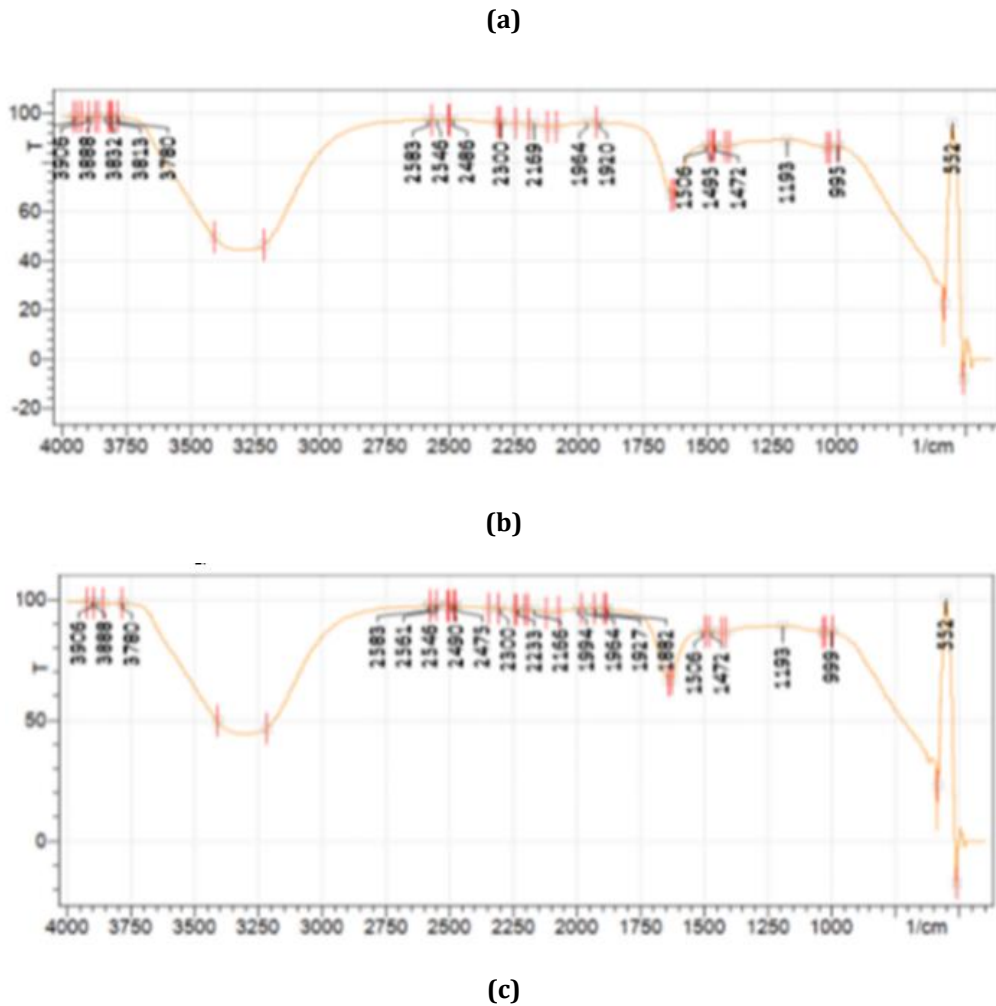
Fig. 2 shows the results of Fourier-Transform Infrared Absorbance Spectra (FTIR) analysis for different weights of seashell powder. Fig. 2(a) shows that the hydroxyapatite is the less dominant compound formed. The spectrum shows absorption of  $(\text{PO}_4^{3-})$  in the region at  $574\text{ cm}^{-1}$ . The broad absorption was also found in the area  $3817\text{ cm}^{-1}$  indicating the presence of the  $\text{OH}^-$  group as a constituent of  $\text{Ca}_{10}(\text{PO}_4)_6(\text{OH})_2$ .

Fig. 2(b) shows that the compound of hydroxyapatite is way better than the previous spectra FTIR HAp synthesis. The spectrum shows absorption of  $(\text{PO}_4^{3-})$  in the region at  $582\text{ cm}^{-1}$ . The strong absorption found in the area of  $3892\text{ cm}^{-1}$  indicates more presence of the  $\text{OH}^-$  group as a constituent of  $\text{Ca}_{10}(\text{PO}_4)_6(\text{OH})_2$ .

Fig. 2(c) shows that hydroxyapatite is the most dominant compound formed. The spectrum shows absorption of  $(\text{PO}_4^{3-})$  in the region at  $694\text{ cm}^{-1}$ . The broad and strong absorption was also found in the area  $4285\text{ cm}^{-1}$  indicating the presence of the  $\text{OH}^-$  group as a constituent of  $\text{Ca}_{10}(\text{PO}_4)_6(\text{OH})_2$ .

In addition, from FTIR analysis for HAp at various weights shows a spectra of phosphate  $(\text{PO}_4^{3-})$  and hydroxyl  $(\text{OH}^-)$  groups. The corresponding peaks of group  $(\text{PO}_4^{3-})$  are witnessed at frequencies of  $470.63\text{ cm}^{-1}$  and  $634.58\text{ cm}^{-1}$ . The  $\text{CO}_2$  is present in uncalcined samples, but it starts to disappear in 20 g, 30 g, and 40 g calcined samples [5]. Since FTIR analysis is meant to detect the functional group of compounds, these results proved that HAp has been produced even with various weight which is 10 g, 20 g and 30 g of seashell powder [6]. All three reactions are slightly common. However, HAp produced at 30 g has an intense phosphate compound around  $552\text{--}558\text{ cm}^{-1}$  compared to 20 g and 10 g of seashell powder. This indicates that HAp produced at 30 g contained higher phosphate ion concentration.





**Fig. 2** Fourier-Transform Infrared Absorbance Spectra (FTIR) analysis of (a) 10g of seashell powder; (b) 20g of seashell powder; (c) 30g of seashell powder

### 3.2 Morphology of HAp in The Effect of Different Weights of Seashell Powder

Scanning Electron Microscope Analysis of HAp is shown in Fig. 3. From the SEM micrographs, the HAp crystals from three conditions were irregular in shape and varied in size. These HAp morphologies were in agreement with previously done studies where the produced HAp have irregular shapes. HAp produced with 10 g, 20 g and 30 g of seashell powder has its difference in the imaging.

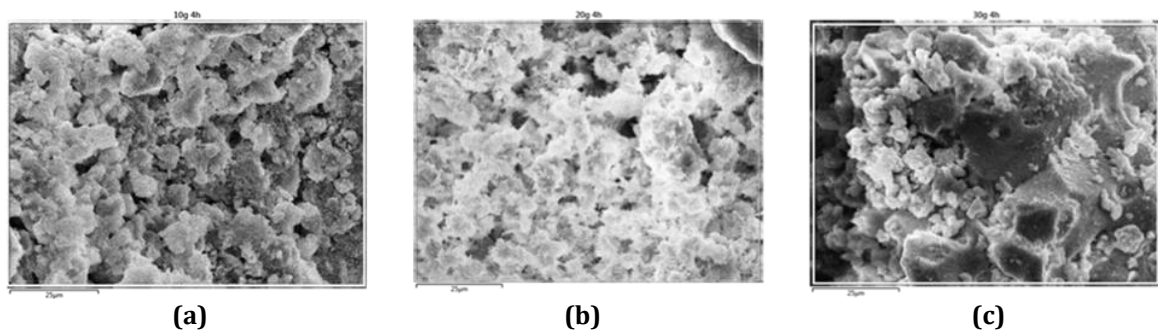


**Fig. 3** SEM Analysis of (a) 10 g of seashell powder, (b) 20 g of seashell powder and (c) 30 g of seashell powder

All three samples of HAp have been imaged under 1000 magnification. The HAp produced with a 30 g reaction time of 4 hours has smaller particles compared to 10 g and 20 g. The increase in weight of the seashell powder has changed the particle size of HAp. There is also more void in HAp containing 30 g seashell powder compared to 20 g and 10 g seashells. It can also clearly be seen that the particles are very compressed in 10 g sample followed by

20 g and 30 g samples. The samples show grain structures which are distinct in nature with obvious grain boundaries evident in the morphology [7]. The interconnectivity between the grain structure becomes closer to each other which typically defines the initiation of a defined crystalline grain structures of hydroxyapatite according to [8]. Hence the sample of 30 g seashell powder produced a denser and smoother surface with various grain structures and boundaries. The distribution of pores is also quite visible in the 30 g sample compared to the 10 g and 20 g samples.

### 3.3 Chemical composition of HAp in The Effect of Different Weights of Seashell Powder

Essentially, the elemental composition of the samples has huge similarities to the chemical composition of natural bone as reported by [9]. Different weight of each element has been detected by using the EDX analyzer. Different weight of each element has been detected by using the EDX analyzer. Table 1 shows the result of the weight percentage of each element for 10 g, 20 g, and 30 g of samples.

**Table 1** Weight of elements

Sample Seashell Powder	Weight of Calcium (%)	Weight of oxygen (%)	Weight of potassium (%)	Weight of Phosphorus (%)	Ca/P Ratio
10g	44.94	26.82	2.18	11.19	4.02
20g	45.68	50.54	0.68	9.80	4.66
30g	64.86	50.42	0.94	13.11	4.94

From Table 1, calculated Ca/p ratios for each sample are 4.02, 4.66 and 4.94 for 10 g, 20 g and 30 g samples. Comparatively the atomic Ca/P ratio (4.02) was the closest to stoichiometric Ca/P ratio of hydroxyapatite (1.67) according to research amongst all the HAp samples investigated in this study. The obtained Ca/P ratios of HAp obtained from this work have a deviation from the theoretical value for pure stoichiometric HAp of 1.67. This is because the weight of calcium detected is large compared to the previous study [10] and the amount of Phosphorus detected is too low. The possible explanation ascribed for large amount of calcium that can be given referring to the past studies is, that seashell might contain more calcium than eggshells [11]. So, the concentration of the phosphorus solution prepared from Potassium dihydrogen phosphate is not enough to get an accurate ratio of HAp. From Table 1, it is also clear that the percentage of oxygen is very high in each sample. This possibly occurred because the Calcium Carbonate has oxidized to Calcium Oxide and this has increased the percentage of oxygen. Therefore, proper precautions have to be taken to reduce the rate of oxidation.

Fig. 4 shows the trend of weight of calcium in percentage and weight of Phosphorus in percentage in the effect of different samples of seashell powder.

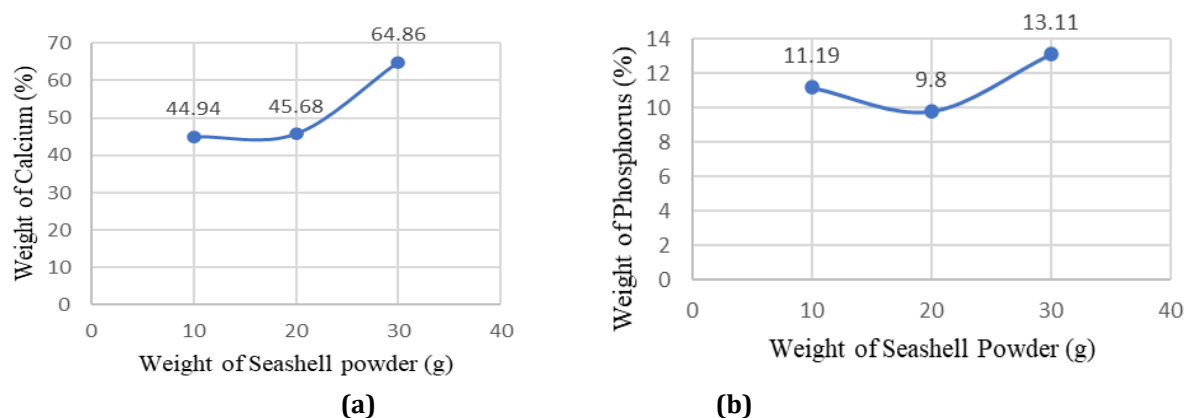


**Fig. 4** Effect of Seashell powder in the weight of (a) Calcium; (b) Phosphorus

### 3.4 X-ray Diffraction analysis

The XRD presents the dominant intensity peaks of  $2\theta$  happened at  $29.37^\circ$  for sample of 10 g of seashell powder,  $29.436^\circ$  for 20 g of seashell powder, and  $29.436^\circ$  for 30 g of seashell powder. No other phases were occurring in this condition. XRD was used for phase identification and characterization of the crystal structures [11]. As indicated in the image, the Hydroxyapatite is more defined, which may be attributed to the increase in size. Because of the amorphous nature of Hydroxyapatite, the peaks blended. With the information provided in Fig. 6, the result shows the presence of 100% of calcium is at peak of  $29.436^\circ$  in 30 g of seashell powder. It was also the

highest peak of Fig. 6 where the composition of seashell was 70%. The calcite peak of 30 g of seashell powder at 29.436 ° is considered as an intermediate product in the conversion of seashell (calcium carbonate) to calcium oxide [12]. The calcite formation can happen faster and may start at temperature of 160-200 °C [13]. The XRD pattern of seashell powder shows the crystal phase with dense peak, higher intensity and sharp resolution. The narrow XRD peak indicated an increase in crystallinity [14], the occurrence of narrow and different XRD shows more crystallinity [15] and the smaller XRD peak shows a lower degree of crystallinity [16]. Hence the higher the weight of seashell powder, the sharper the intensity (crystallinity increases) in the diffraction image [17], [18].

#### 4. Conclusion

The results obtained from all the characterization techniques confirm that HAp is synthesized from CaO, employed as a precursor extracted from seashell waste. The synthesis and characterization of hydroxyapatite using a precursor extracted from seashell waste can be a promising approach with several advantages. The XRD result reveals the crystallinity and the FTIR analysis evidences the phase purity of HAp powder. From the SEM test of hydroxyapatite powder the ratio of Ca and P was found around 4.02. This is in an acceptable range, as in the ideal HAp the weight ratio of Ca and P is 1.67. The obtained Ca/P ratios of HAp obtained from this work have deviation from the theoretical value for pure stoichiometric HAp of 1.67. This is because previous researches does not state the concentration of potassium dihydrogen phosphate but for this work 29.98 mg/L of  $\text{KH}_2\text{PO}_4$  was used to extract the HAp from a seashell. Therefore, increasing the concentration of phosphorus in the synthesis of HAp might lead to a higher content of phosphate in the final product. During the characterization, work efficiently and conduct measurements promptly to minimize exposure of the samples to air. This is particularly important for techniques such as XRD or SEM where prolonged exposure to oxygen can lead to surface oxidation and potential changes in the observed properties. In conclusion, the weight of seashell powder is an important parameter in HAp production. Further research and optimization of the synthesis process will enhance the understanding and utilization of seashell waste as a precursor for hydroxyapatite synthesis.

#### Acknowledgement

This research was supported by Universiti Tun Hussein Onn Malaysia (UTHM) through Tier 1 (vot Q521). The authors would also like to thank the Centre for Diploma Studies, Universiti Tun Hussein Onn Malaysia for its support.

#### Conflict of Interest

Authors declare that there is no conflict of interests regarding the publication of the paper.

#### Author Contribution

*The authors confirm contribution to the paper as follows: **study conception and design:** Posharani Saravanan, Sharrmitah Saravanakumar, Rozainita Rosley; **data collection:** Posharani Saravanan, Sharrmitah Saravanakumar, Rozainita Rosley; **analysis and interpretation of results:** Posharani Saravanan, Sharrmitah Saravanakumar, Rozainita Rosley; **draft manuscript preparation:** Posharani Saravanan, Sharrmitah Saravanakumar, Rozainita Rosley. All authors reviewed the results and approved the final version of the manuscript.*

#### References

- [1] Rehman, M. U., Qureshi, A., & Baloch, M. M. (2021). Extraction of Hydroxyapatite from Caprine Bones and its Anti-Bacterial Study. *Mehran University Research Journal of Engineering and Technology*, 40(4), 867–873. <https://doi.org/10.22581/muet1982.2104.16>
- [2] Bi, Y., Lin, Z., & Deng, S. (2019). Fabrication and characterization of hydroxyapatite/sodium alginate/chitosan composite microspheres for drug delivery and bone tissue engineering. *Materials Science and Engineering: C*, 100, 576–583. <https://doi.org/10.1016/j.msec.2019.03.040>
- [3] Kumar, C. S., Dhanaraj, K., Vimalathithan, R., Ilaiyaraja, P., & Suresh, G. (2020). Hydroxyapatite for bone related applications derived from sea shell waste by simple precipitation method. *Journal of Asian Ceramic Societies*, 8(2), 416–429. <https://doi.org/10.1080/21870764.2020.1749373>
- [4] Farombi, A. G., Amuda, O. S., Alade, A. O., Okoya, A. A., & Adebisi, S. A. (2018). Central composite design for optimization of preparation conditions and characterization of hydroxyapatite produced from catfish bones. *Beni-Suef University Journal of Basic and Applied Sciences*, 7(4), 474–480. <https://doi.org/10.1016/j.bjbas.2018.04.005>

- [5] Synthesis and Characterizations of Hydroxyapatite using Precursor Extracted from Chicken Egg Shell Waste. (2021). *Biointerface Research in Applied Chemistry*, 12(4), 5663–5671. <https://doi.org/10.33263/briac124.56635671>
- [6] Synthesis of hydroxyapatite from cockle shell wastes. (n.d.). CORE Reader. <https://core.ac.uk/reader/188217070>
- [7] Ooi, C. Y., Hamdi, M., & Ramesh, S. (2007). Properties of hydroxyapatite produced by annealing of bovine bone. *Ceramics International*, 33(7), 1171–1177. <https://doi.org/10.1016/j.ceramint.2006.04.001>
- [8] Obada, D. O., Dauda, E., Abifarin, J. K., Dodoo - Arhin, D., & Bansod, N. D. (2020). Mechanical properties of natural hydroxyapatite using low cold compaction pressure: Effect of sintering temperature. *Materials Chemistry and Physics*, 239, 122099. <https://doi.org/10.1016/j.matchemphys.2019.122099>
- [9] Haberkowicz, K., Bućko, M. M., Brzezińska-Miecznik, J., Haberkowicz, M., Mozgawa, W., Panz, T., Pyda, A., & Zarębski, J. (2006). Natural hydroxyapatite—its behaviour during heat treatment. *Journal of the European Ceramic Society*, 26(4–5), 537–542. <https://doi.org/10.1016/j.jeurceramsoc.2005.07.033>
- [10] Lee, S. W., Balázs, C., Balázs, K., Seo, D. H., Kim, H. S., Kim, C. H., & Kim, S. (2014). Comparative Study of hydroxyapatite prepared from seashells and eggshells as a bone graft material. *Tissue Engineering and Regenerative Medicine*, 11(2), 113–120. <https://doi.org/10.1007/s13770-014-0056-1>
- [11] Dahlan. (2006). Characterisation Cluster Bone Phosphate and Carbonate In Mice with Fourier Transform Infrared (FT-IR) Spectroscopy. *Ind. J. Mat. Sci*, 12, 221–224.
- [12] Synthesis and characterization of hydroxyapatite from bulk seashells and its potential usage as lead ions adsorbent. (2017). *The Malaysian Journal of Analytical Sciences*, 21(3). <https://doi.org/10.17576/mjas-2017-2103-07>
- [13] Pederson, C. L., Mavromatis, V., Dietzel, M., Rollion - Bard, C., Nehrke, G., Jöns, N., Jochum, K. P., & Immenhauser, A. (2019). Diagenesis of mollusc aragonite and the role of fluid reservoirs. *Earth and Planetary Science Letters*, 514, 130–142. <https://doi.org/10.1016/j.epsl.2019.02.038>
- [14] Okada, M., Fujiwara, K., Uehira, M., Matsumoto, N., & Shoji, T. (2013). Expansion of nanosized pores in low-crystallinity nanoparticle-assembled plates via a thermally induced increase in solid-state density. *Journal of Colloid and Interface Science*, 405, 58–63. <https://doi.org/10.1016/j.jcis.2013.05.022>
- [15] Karamian, E., Khandan, A., Eslami, M., Gheisari, H., & Rafiaei, N. (2013). Investigation of HA Nanocrystallite Size Crystallographic Characterizations in NHA, BHA and HA Pure Powders and their Influence on Biodegradation of HA. *Advanced Materials Research*, 829, 314–318. <https://doi.org/10.4028/www.scientific.net/amr.829.314>
- [16] Locardi, B., Pazzaglia, U., Gabbi, C., & Profilo, B. (1993). Thermal behaviour of hydroxyapatite intended for medical applications. *Biomaterials*, 14(6), 437–441. [https://doi.org/10.1016/0142-9612\(93\)90146-s](https://doi.org/10.1016/0142-9612(93)90146-s)
- [17] Zuliantoni, Suprpto, W., Setyarini, P. H., & Sanjay, M. R. (2022). Extraction and characterization of snail shell waste hydroxyapatite. *Results in Engineering*, 14, 100390. <https://doi.org/10.1016/j.rineng.2022.100390>
- [18] characterization of hydroxyapatite synthesized from biowastes. *Data in Brief*, 26, 104485. <https://doi.org/10.1016/j.dib.2019.104485>